Mechanical Stresses in a Linear Plastic FGM Hollow Cylinder Due to Non-Axisymmetric Loads

M. Shokouhfar [*] , M. Jabbari

South Tehran Branch, Islamic Azad University,Tehran, Iran

ABSTRACT

In this paper, an analytical solution for computing the linear plastic stresses and critical pressure in a FGM hollow cylinder under the internal pressure due to non-Axisymmetric Loads is developed. It has been assumed that the modulus of elasticity was varying through thickness of the FGM material according to a power law relationship. The Poisson's ratio was considered constant throughout the thickness. The general form of mechanical boundary conditions is considered on the inside surfaces. In the analysis presented here the effect of non-homogeneity in FGM cylinder was implemented by choosing a dimensionless parameter, named m, which could be assigned an arbitrary value affecting the stresses in the cylinder. Distribution of stresses in radial, circumferential and shear directions for FGM cylinders under the influence of internal pressure were obtained. Graphs of variations of stress versus radius of the cylinder were plotted. The direct method is used to solve the Navier equations. © 2016 IAU, Arak Branch.All rights reserved.

Keywords : Hollow cylinder; Non-Homogenous; Non- Axisymmetri; FGM; Elastic-plastic analysis.

1 INTRODUCTION

FUNCTIONALLY graded material (FGM) is heterogeneous material in which the elastic and thermal properties change from one surface to the other, gradually and continuously. Since ceramic has good resistance to heat, corrosion, and erosion and metal has high fracture toughness, ceramic-metal FGM may work at super high-temperatures or under high temperature differences and also corrosive fields. In effect, the governing equations of temperature and stress distributions are coordinate dependent as the material properties are functions of position.

There are a number of analytical thermal and mechanical stress calculations for functionally graded material in the one-dimensional case for thick cylinders and spheres [1, 2]. The authors have considered non-homogeneous material properties as linear function of radius. Jabbari et al. [3] presented a general solution for mechanical and thermal stresses in a functionally graded hollow cylinder due to non-axisymmetric steady-state load. They applied separation of variables and complex Fourier series to solve the heat conduction and Navier equations. Poultangari et al. [4] presented a solution for the functionally graded hollow spheres under non-axisymmetric thermo-mechanical loads. Lu yunbing et al. [5] analyzed the steady state temperature distribution and the associated thermal stress distribution of a 3-layer composite cylinder system with material ingredient changing continuously in the middle FGM layer and a set of formulas for the temperature and the thermal stresses are obtained. Shariyat et al. [6] presented the nonlinear transient thermal stress and elastic wave propagation of thick temperature-dependent FGM cylinders, using a second-order point-collocation method. In another work [7], he found an algorithm for nonlinear

_____

[*]Corresponding author.
E-mail address: miladshokouhfar@gmail.com (M.Shokouhfar).

transient behavior analysis of thick functionally graded cylindrical vessels or pipes with temperature-dependent material properties under thermo-mechanical load. Chen and Lim [8] presented elastic mechanical behavior of nano-scaled FGM films incorporating surface energies. Afsar and Sekine [9] presented inverse problems of material distributions for prescribed apparent fracture toughness in FGM coatings around a circular hole in infinite elastic media. Tajeddini et al. [10] discussed the three-dimensional free vibration of thick circular and annular isotropic and functionally graded (FG) plates with variable thickness along the radial direction. Nosier and Fallah [11], based on the first-order shear deformation plate theory with the von Karman non-linearity, presented the non-linear axisymmetric and asymmetric behavior of functionally graded circular plates under transverse mechanical loading. Zhang and Zhou [12] conducted a theoretical analysis of FGM thin plates based on the physical neutral surface. Fazelzadeh and Hosseini [13] discussed the aero-thermoelastic behavior of supersonic rotating thin-walled beams made of functionally graded materials. Ootao and Tanigawa [14] analyzed the transient thermo elastic problem of functionally graded thick strip due to non-uniform heat supply. They obtained the exact solution for the two-dimensional temperature change in a transient state, and thermal stresses of a simply supported strip under the state of plane strain condition. Jabbari et al. [15] studied the mechanical and thermal stresses in functionally graded hollow cylinder due to radial symmetric loads. They assumed the temperature distribution to be a function of radial direction. They applied a direct method to solve the heat conduction and Navier equations. Farid et al. [16] presented three-dimensional temperature dependent free vibration analysis of functionally graded material curved panels resting on two-parameter elastic foundation using a hybrid semi-analytic differential quadrature method. Bagri and Eslami [17] analyzed the generalized coupled thermoelasticity of functionally graded annular disk considering the Lord–Shulman theory. Jabbari et al [18] studied an axisymmetric mechanical and thermal stresses in a thick short length functionally graded material cylinder. They applied separation of variables and complex Fourier series to solve the heat conduction and Navier equation. Zamani-nejad and Rahimi [19], using the infinitesimal theory of elasticity, derived closed-form solutions for the one-dimensional steady-state thermal stresses in a rotating functionally graded (FGM) pressurized thick-walled hollow circular cylinder under generalized plane strain and plane stress assumptions, respectively. Batra and Iaccarino [20] found closed-form solutions for axisymmetric plane strain deformations of a functionally graded circular cylinder comprised of an isotropic and incompressible second-order elastic material with elastic module varying only in the radial direction. Cylinder's inner and outer surfaces are loaded by hydrostatic pressures. Three-dimensional thermo-elastic analysis of a functionally graded cylindrical panel with finite length and subjected to non-uniform mechanical and steady-state thermal loads are carried out by Shao and Wang [21].

There are limited papers on the subject of plasticity of FGM structures. Shabana and Noda [22] presented thermo-elasto-plastic stresses in functionally graded materials subjected to thermal loading taking residual stresses of the fabrication process into consideration. Eraslan and Akis [23] presented plane strain analytical solutions for a functionally graded elastic–plastic pressurized tube. Eraslan and Arslan [24] discussed the plasticity of plane strain rotating graded hollow shafts. The elasto-plastic response of a long functionally graded tube subjected to internal pressure is given by Eraslan and Akis [25]. Alla et al. [26] analyzed the elastic–plastic problem of 2D-FGM plates made of ZrO2, 6061-T6 and Ti-6Al-4V under transient thermal loading. Lu [27] presented a stress analysis for the functionally graded disc under mechanical loads and a steady state temperature distribution. Jahromi [28] obtained the elasto-plastic stresses in a functionally graded rotating disk. Sadeghian and Toussi [29] presented the elasto-plastic axisymmetric thermal stress analysis of functionally graded cylindrical vessel.

Classical method of analysis is to combine the equilibrium equations with the stress-strain and strain-equilibrium equations relations to arrive at the governing equation in terms of the displacement components called the Navier equation. Navier equations are solved in elastic and plastic hollow FGM, analytically. The analysis is presented for two types of applicable boundary conditions. In this work, an analytical method is presented for linear plastic mechanical stress analysis for a hollow cylinder made of functionally graded materials. Mechanical boundary conditions are considered in general forms. It has been assumed that the modulus of elasticity was varying through thickness of the FGM material according to a power law relationship. The Poisson's ratio was considered constant throughout the thickness. The Navier equation is solved analytically by the direct method.

2 EQUATIONS

The linear plastic stress–strain relations for plane-strain conditions are

$$\sigma_{rr}=(\lambda+2\mu)\ (\varepsilon_{rr}+\epsilon_{rr}^{p})+\lambda(\varepsilon_{\theta\theta}+\varepsilon_{\theta\theta}^{p}),\qquad \sigma_{\theta\theta}=(\lambda+2\mu)(\varepsilon_{\theta\theta}+\varepsilon_{\theta\theta}^{p})+\lambda(\varepsilon_{rr}+\epsilon_{rr}^{p}),\qquad \sigma_{r\theta}=2\mu(\varepsilon_{r\theta}+\varepsilon_{r\theta}^{p})$$

$$(\varepsilon_{rr}^{p}+\varepsilon_{\theta\theta}^{p})=0,\qquad \varepsilon_{rr}=u_{,r},\qquad \varepsilon_{\theta\theta}=\frac{u}{r}+\frac{v_{,\theta}}{r},\qquad \varepsilon_{r\theta}=\frac{1}{2}(\frac{u_{,\theta}}{r}+v_{,r}-\frac{v}{r}),\qquad \varepsilon_{r\theta}^{p}=\frac{3\epsilon\Delta\epsilon_{\rho}S_{ij}}{\sigma_{0}}$$

$$\Delta\varepsilon_{\rho}=\frac{\sqrt{2}}{3}\left[\left(\varepsilon_{rr}^{p}-\varepsilon_{\theta\theta}^{p}\right)^{2}+\varepsilon_{rr}^{p\,2}+\varepsilon_{\theta\theta}^{p\,2}+6\varepsilon_{r\theta}^{p\,2}\right]^{2}$$

(1)

where $(,r)$ denotes differentiation with respect to r and (ε^{p}) means plastic strain described at linear plastic strain part. Where σ_{ij} and $\varepsilon_{ij}\,(i,j=r,\theta)$ are the stress and strain tensors, λ and μ are Lame′ coefficients related to the modulus of elasticity E and Poisson's ratio v as:

$$\lambda=\frac{vE}{(1+v)(1-2v)}\qquad\qquad \mu=\frac{E}{2(1+2v)}$$

(2)

The equilibrium equation in the radial direction, disregarding the body force and the inertia term, is

$$\sigma_{rr,r}+\frac{1}{r}\sigma_{r\theta,\theta}+(\frac{\sigma_{rr}-\sigma_{\theta\theta}}{r})=0\qquad\qquad \sigma_{r\theta,r}+\frac{1}{r}\sigma_{\theta\theta,\theta}+\frac{2}{r}\sigma_{r\theta}=0$$

(3)

To yield the equation of stresses in terms of plastic strain for the FGM cylinder, the functional relationship of the material properties must be known. Since the cylinder's material is assumed to be graded along the r direction, the modulus of elasticity, the coefficient of thermal expansion and yield strength are assumed to be described with a power law as:

$$E=E_{0}(\frac{r}{l})^{m_{1}}=E_{0}\,\mathrm{r}^{m_{1}}\qquad\qquad \alpha=\alpha_{0}(\frac{r}{l})^{m_{2}}=\alpha_{0}\,\mathrm{r}^{m_{2}}\qquad\qquad \sigma=\sigma_{0}(\frac{r}{l})^{m_{4}}=\sigma_{0}\,\mathrm{r}^{m_{4}}$$

(4)

where E_{0} and α_{0} are the material constants and m_{1},m_{2},m_{3} and m_{4} are the power law indices of the material and σ_{0r} is yielding point. We may further assume that Poisson's ratio is constant.

2.1 Linear plastic strain

The elastic stresses are [3]

$$\sigma_{rr}=\frac{E_{0}}{(1-v)(1-2v)}([\sum_{j=1}^{2}((1-v)\eta_{0j}+v)B_{0j}r^{\eta_{0j}+m_{1}-1}+\sum_{n=-\infty,n\neq0}^{\infty}\left[(\sum_{j=1}^{4}[(1-v)\eta_{nj}+v(inN_{nj}+1)]B_{nj}r^{\eta_{nj}+m_{1}-1})\right]e^{in\theta})]$$

(5)

$$\sigma_{\theta\theta}=\frac{E_{0}}{(1-v)(1-2v)}([\sum_{j=1}^{2}((1-v)+v\eta_{0j})B_{0j}r^{\eta_{0j}+m_{1}-1}+\sum_{n=-\infty,n\neq0}^{\infty}\left[(\sum_{j=1}^{4}[(1-v)(inN_{nj}+1)+v\eta_{nj}]B_{nj}r^{\eta_{nj}+m_{1}-1})\right]e^{in\theta})]$$

(6)

$$\sigma_{r\theta}=\frac{E_{0}}{2(1+v)}([\sum_{j=3}^{4}(\eta_{0j}-1)B_{0j}r^{\eta_{0j}+m_{1}-1}+\sum_{n=-\infty,n\neq0}^{\infty}\left[(\sum_{j=1}^{4}[(in+\eta_{nj}\,N_{nj}-N_{nj})]B_{nj}r^{\eta_{nj}+m_{1}-1})\right]e^{in\theta})]$$

(7)

Based on the graph of (ε_{rr}^{p},S) the gradient $(M*E)$ of graph yields, so the equation of linear plastic strain for mechanical stresses based on this graph obtains as [30]

$$\varepsilon_{rr}^p = \frac{1-M}{M}(1-S) \qquad S = s_{\theta\theta} - s_{rr} \qquad s_{rr} = \frac{\sigma_{rr}}{\sigma_0 r^{m_4}} \qquad s_{\theta\theta} = \frac{\sigma_{\theta\theta}}{\sigma_0 r^{m_4}} \qquad s_{r\theta} = \frac{\sigma_{r\theta}}{\sigma_0 r^{m_4}} \tag{8}$$

From Eq. (8), S and $s_{r\theta}$ yield as:

$$S = (\frac{E_0}{(1-v)(1-2v)\sigma_0}([\sum_{j=1}^{2}(1-2v+2v\eta_{0j}-\eta_{0j})B_{0j}r^{\eta_{0j}+m_1-1-m_4}$$
$$+ \sum_{n=-\infty,n\neq 0}^{\infty}\left[(\sum_{j=1}^{4}[inN_{nj}-2vinN_{nj}+1-2v+2v\eta_{nj}-\eta_{nj}]B_{nj}r^{\eta_{nj}+m_1-1-m_4})\right]e^{in\theta})]) \tag{9}$$

$$s_{r\theta} = \frac{E_0}{2(1+v)\sigma_0}([\sum_{j=3}^{4}(\eta_{0j}-1)B_{0j}r^{\eta_{0j}+m_1-1-m_4} + \sum_{n=-\infty,n\neq 0}^{\infty}\left[(\sum_{j=1}^{4}[(in+\eta_{nj}\ N_{nj}-N_{nj})]B_{nj}r^{\eta_{nj}+m_1-1-m_4})\right]e^{in\theta})]$$

By substituting Eq. (9) into Eq. (8) the ε_{rr}^p yields

$$\varepsilon_{rr}^p = (\frac{1-M}{M})\left(1-(\frac{E_0}{(1-v)(1-2v)\sigma_0}([\sum_{j=1}^{2}(1-2v+2v\eta_{0j}-\eta_{0j})B_{0j}r^{\eta_{0j}+m_1-1-m_4}\atop + \sum_{n=-\infty,n\neq 0}^{\infty}\left[(\sum_{j=1}^{4}[inN_{nj}-2vinN_{nj}+1-2v+2v\eta_{nj}-\eta_{nj}]B_{nj}r^{\eta_{nj}+m_1-1-m_4})\right]e^{in\theta})])\right) \tag{10}$$

From Eq. (8) the $\varepsilon_{rr,r}^p$ and $\varepsilon_{rr,rr}^p$ yield as:

$$\varepsilon_{rr,r}^p = \frac{1-M}{M}(1-S_{,r}) \qquad \varepsilon_{rr,rr}^p = \frac{1-M}{M}(1-S_{,rr}) \tag{11}$$

By substituting Eq. (9) into Eq. (1) the $\varepsilon_{r\theta}^p$ yields

$$\varepsilon_{r\theta}^p = \frac{3\epsilon\Delta\epsilon_\rho E_0}{2(1+v)\sigma_0}([\sum_{j=3}^{4}(\eta_{0j}-1)B_{0j}r^{\eta_{0j}+m_1-1-m_4} + \sum_{n=-\infty,n\neq 0}^{\infty}\left[(\sum_{j=1}^{4}[(in+\eta_{nj}\ N_{nj}-N_{nj})]B_{nj}r^{\eta_{nj}+m_1-1-m_4})\right]e^{in\theta})] \tag{12}$$

$$\Delta\epsilon_\rho = \frac{\sqrt{2}}{3}\left[\left(\epsilon_{rr}^p-\epsilon_{\theta\theta}^p\right)^2+\epsilon_{rr}^{p\,2}+\epsilon_{\theta\theta}^{p\,2}+6\epsilon_{r\theta}^{p\,2}\right]^2 \qquad \varepsilon_{r\theta,\theta}^p = \varepsilon_{rr,\theta}^p = 0$$

2.2 Linear plastic stresses

With using relations (1) to (4), the Navier equations in term of the displacements are

$$U_{,rr} +(m_1+1)\ \frac{1}{r}U_{,r}+(\frac{vm_1}{1-v}-1)\frac{1}{r^2}U+(\frac{1-2v}{2-2v})\frac{1}{r^2}U_{,\theta\theta}+(\frac{1}{2-2v})\frac{1}{r}V_{,r\theta}+(\frac{v(4+2m_1)-3}{2-2v})\frac{1}{r^2}V_{,\theta} =$$
$$-\epsilon_{rr,r}^p -(\frac{1}{2-2v})\frac{1}{r}\epsilon_{r\theta,\theta}^p-(\frac{1-2v+m_1(1-v)}{2-2v})\frac{1}{r}\epsilon_{rr}^p+(\frac{v}{1-v})\frac{1}{r}\epsilon_{\theta\theta,r}^p-(\frac{v(2+m_1)-1}{1-v})\frac{1}{r}\epsilon_{\theta\theta}^p$$

$$V_{,rr} +(m_1+1)\ \frac{1}{r}V_{,r}+(m_1-1)\frac{1}{r^2}V+(\frac{2-2v}{1-2v})\frac{1}{r^2}V_{,\theta\theta}+(\frac{1}{1-2v})\frac{1}{r}U_{,r\theta}+(\frac{3-4v}{1-2v}+m_1)\frac{1}{r^2}U_{,\theta} = \tag{13}$$
$$-\epsilon_{r\theta,r}^p -(2+m_1)\frac{1}{r}\epsilon_{r\theta}^p-(\frac{1-v}{1-2v})\frac{1}{r}\epsilon_{\theta\theta,r}^p+(\frac{2v}{1-2v})\frac{1}{r}\epsilon_{rr,\theta}^p$$

To solve the Navier equations, the displacement components $U(r,)$ and $V(r,)$ are expanded in the complex Fourier series as:

$$u(r,\theta) = \sum_{n=-\infty}^{\infty} u_n(r)e^{in\theta} \qquad v(r,\theta) = \sum_{n=-\infty}^{\infty} v_n(r)e^{in\theta} \tag{14}$$

where $u_n(r)$ and $v_n(r)$ are the coefficients of complex Fourier series of $u(\mathrm{r},\theta)$ and $v(\mathrm{r},\theta)$ respectively, and are

$$u_n(r) = \frac{1}{2\pi}\int_{-\pi}^{\pi} u(r,\theta)e^{-in\theta}d\theta \qquad v_n(r) = \frac{1}{2\pi}\int_{-\pi}^{\pi} \mathrm{v}(r,\theta)e^{-in\theta}d\theta \tag{15}$$

The Fourier series for 1 is

$$1 = \sum_{n=-\infty}^{\infty} \frac{i}{2\pi n}(e^{-in\pi} - e^{in\pi})e^{in\theta} \tag{16}$$

By substituting Eq. (14), Eq. (15) and Eq. (16) into Eq. (13) the $U_n^{''}$ and $V_n^{''}$ yield as:

$$U_n^{''} + (m_1+1)\frac{1}{r}U_n^{'} + (\frac{\nu m_1}{1-\nu}-1-\frac{(1-2\nu)n^2}{2-2\nu})\frac{1}{r^2}U_n + (\frac{in}{2-2\nu})\frac{1}{r}V_n^{'} + in(\frac{\nu(4+2m_1)-3}{2-2\nu})\frac{1}{r^2}V_n =$$
$$(\frac{2\nu-1}{1-\nu})\varepsilon_{rm,r}^p + (\frac{2\nu m_1+4\nu-m_1-2}{1-\nu})\frac{1}{r}\varepsilon_{rm}^p \tag{17}$$

$$V_n^{''} + (m_1+1)\frac{1}{r}V_n^{'} + (m_1+1+\frac{(2-2\nu)n^2}{1-2\nu})\frac{1}{r^2}V_n + (\frac{in}{2-2\nu})\frac{1}{r}U_n^{'} + in(\frac{(3-4\nu)}{1-2\nu}+m_1)\frac{1}{r^2}U_n =$$
$$-\varepsilon_{r\theta n,r}^p - (m_1+2)\frac{1}{r}\varepsilon_{r\theta n}^p \tag{18}$$

Eqs. (17) and (18) are a system of ordinary differential equations having general and particular solutions. The general solutions are assumed as:

$$u_n^g = Br^\eta \qquad v_n^g = Cr^\eta \tag{19}$$

Substituting Eq. (19) into Eq. (17) and (18), yields

$$\left[\eta(\eta-1)+\eta(m_1+1)+\frac{\nu m_1}{1-\nu}-1-\frac{(1-2\nu)n^2}{2-2\nu}\right]B + i\left[\frac{\eta}{2-2\nu}+(\frac{\nu(4+2m_1)-3}{2-2\nu})\right]nC = 0$$

$$\left[\eta(\eta-1)+\eta(m_1+1)-m_1-1-\frac{(2-2\nu)n^2}{1-2\nu}\right]C + i\left[\frac{\eta}{1-2\nu}+(\frac{3-4\nu}{1-2\nu})+m_1\right]nB = 0 \tag{20}$$

A nontrivial solution of Eq. (20) yields as:

$$\left[\eta(\eta-1)+\eta(m_1+1)+\frac{\nu m_1}{1-\nu}-1-\frac{(1-2\nu)n^2}{2-2\nu}\right]\left[\eta(\eta-1)+\eta(m_1+1)-m_1-1-\frac{(2-2\nu)n^2}{1-2\nu}\right]+$$

$$n^2\left[\frac{\eta}{2-2\nu}+(\frac{\nu(4+2m_1)-3}{2-2\nu})\right]\left[\frac{\eta}{1-2\nu}+(\frac{3-4\nu}{1-2\nu})+m_1\right] = 0 \tag{21}$$

Eq. (21) has four roots η_{n1} to η_{n4}. So, the general solutions are

$$u_n^g = \sum_{j=1}^{4} B_{nj}r^{\eta_{nj}} \qquad v_n^g = \sum_{j=1}^{4} N_{nj}C_{nj}r^{\eta_{nj}} \tag{22}$$

where N_{nj} is the relation between constants B_{nj} and C_{nj} yielded from the first of Eq. (21) as:

$$N_{nj} = \frac{i\left[\eta_{nj}(\eta_{nj}-1)+\eta_{nj}(m_1+1)+\frac{vm_1}{1-v}-1-\frac{n^2(1-2v)}{2-2v}\right]}{n\left[\frac{\eta_{nj}}{2-2v}+\frac{v(4+2m_1)-3}{2-2v}\right]} \qquad j=1,2,3,4 \qquad (23)$$

For isotropic materials ($m_1=0$) and for $n=1$, Eq. (23) has repeated roots so hence a solution of the form of Lnr must be considered for u_1^g and v_1^g.

The particular solutions $u_n^p(r)$ and $v_n^p(r)$ are assumed as:

$$u_n^p = I_{n1}r^2 + I_{n2}r \qquad v_n^p = I_{n3}r^2 + I_{n4}r \qquad (24)$$

By substituting Eq. (24) into Eq. (17) and Eq. (18) the I_{nj} yields as:

$$I_{n1} = \frac{g_{15}g_5\varepsilon_{rr,r}^p + g_{13}\varepsilon_{r\theta,r}^p}{g_{15}g_{11}-g_{13}g_{17}} \qquad I_{n2} = \frac{g_{16}g_6\varepsilon_{rr}^p - g_{10}g_{14}\varepsilon_{r\theta}^p}{g_{12}g_{16}-g_{14}g_{18}}$$

$$I_{n3} = \frac{g_{11}\varepsilon_{r\theta,r}^p + g_{17}g_5\varepsilon_{rr,r}^p}{g_{17}g_{13}-g_{11}g_{15}} \qquad I_{n4} = \frac{g_6g_{18}\varepsilon_{rr}^p - g_{10}g_{12}\varepsilon_{r\theta}^p}{g_{14}g_{18}-g_{12}g_{16}} \qquad (25)$$

The coefficients of g_1 to g_{18} formula presented at Appendix part (A).

The complete solutions for $u_n(r)$ and $v_n(r)$ are the sum of the general and particular solutions as:

$$u_n(r) = \sum_{j=1}^{4} B_{nj}r^{\eta_{nj}} + I_{n1}r^2 + I_{n2}r \qquad v_n(r) = \sum_{j=1}^{4} N_{nj}B_{nj}r^{\eta_{nj}} + I_{n3}r^2 + I_{n4}r \qquad (26)$$

For $n=0$ the coefficient N_{nj} in Eq. (23) is undefined because the system of Eq. (17) and (18) for $n=0$ is two decoupled ordinary differential equations as:

$$U_0'' + (m_1+1)\frac{1}{r}U_0' + (\frac{vm_1}{1-v}-1)\frac{1}{r^2}U_0 = g_5\varepsilon_{rr0,r}^p + g_6\frac{1}{r}\varepsilon_{rr0}^p$$

$$V_0'' + (m_1+1)\frac{1}{r}V_0' + (m_1+1)\frac{1}{r^2}V_0 = -\varepsilon_{r\theta0,r}^p + g_{10}\frac{1}{r}\varepsilon_{r\theta0}^p \qquad (27)$$

The solutions of Eq. (27) are

$$u_0(r) = \sum_{j=1}^{2} B_{0j}r^{\eta_{0j}} + I_{01}r^2 + I_{02}r \qquad v_0(r) = \sum_{j=3}^{4} B_{0j}r^{\eta_{0j}} + I_{03}r^2 \qquad (28)$$

$$\eta_{01,2} = -\frac{m_1}{2} \pm (\frac{m_1^2}{4}-\frac{vm_1}{1-v}+1)^{.5} \qquad \eta_3 = 1 \qquad \eta_4 = -(m_1+1)$$

$$I_{01} = \frac{g_5\varepsilon_{rr0,r}^p}{2(2+m_1)+(\frac{vm_1}{1-v}-1)} \qquad I_{02} = \frac{g_6\varepsilon_{rr0}^p}{(\frac{vm_1}{1-v}+m_1)} \qquad I_{03} = -\frac{\varepsilon_{r\theta0,r}^p}{(5+3m_1)} \qquad (29)$$

By substituting Eq. (28) and (26) into Eq. (14) the $u(r,\theta)$ and $v(r,\theta)$ yield as:

$$u(r,\theta) = \sum_{j=1}^{2} B_{0j} r^{\eta_{0j}} + I_{01} r^2 + I_{02} r + \sum_{n=-\infty, n\neq 0}^{\infty} \left[(\sum_{j=1}^{4} B_{nj} r^{\eta_{nj}}) + I_{n1} r^2 + I_{n2} r \right] e^{in\theta}$$

$$v(r,\theta) = \sum_{j=3}^{4} B_{0j} r^{\eta_{0j}} + I_{03} r^2 + \sum_{n=-\infty, n\neq 0}^{\infty} \left[(\sum_{j=1}^{4} N_{nj} B_{nj} r^{\eta_{nj}}) + I_{n3} r^2 + I_{n4} r \right] e^{in\theta}$$

(30)

Substituting Eq. (30) into Eq. (1), the linear plastic stresses yield as:

$$\sigma_{rr} = \frac{E_0}{(1-v)(1-2v)}([\sum_{j=1}^{2}((1-v)\eta_{0j}+v)B_{0j} r^{\eta_{0j}+m_1-1} + (2-v)I_{01} r^{m_1+1} + I_{02} r^{m_1} + (1-v)(I_{01,r} r^{m_1+2} + I_{02,r} r^{m_1+1})$$

$$+ \sum_{n=-\infty, n\neq 0}^{\infty} \left[\begin{array}{l} (\sum_{j=1}^{4}[(1-v)\eta_{nj}+v(inN_{nj}+1)]B_{nj} r^{\eta_{nj}+m_1-1}) + (2-v)I_{n1} r^{m_1+1} + I_{n2} r^{m_1} + (vin)I_{n3} r^{m_1+1} \\ +(vin)I_{n4} r^{m_1} + (1-v)I_{n1,r} r^{m_1+2} + I_{n2,r} r^{m_1+1}) \end{array} e^{in\theta} \right)]$$

(31)

$$\sigma_{\theta\theta} = \frac{E_0}{(1-v)(1-2v)}([\sum_{j=1}^{2}((1-v)+v\eta_{0j})B_{0j} r^{\eta_{0j}+m_1-1} + (1+v)I_{01} r^{m_1+1} + I_{02} r^{m_1} + v(I_{01,r} r^{m_1+2} + I_{02,r} r^{m_1+1})$$

$$+ \sum_{n=-\infty, n\neq 0}^{\infty} \left[\begin{array}{l} (\sum_{j=1}^{4}[(1-v)(inN_{nj}+1)+v\eta_{nj}]B_{nj} r^{\eta_{nj}+m_1-1}) + (1+v)I_{n1} r^{m_1+1} + I_{n2} r^{m_1} + in(1-v)I_{n3} r^{m_1+1} \\ +in(1-v)I_{n4} r^{m_1} + v(I_{n1,r} r^{m_1+2} + I_{n2,r} r^{m_1+1}) \end{array} e^{in\theta} \right)]$$

(32)

$$\sigma_{r\theta} = \frac{E_0}{2(1+v)}([\sum_{j=3}^{4}(\eta_{0j}-1)B_{0j} r^{\eta_{0j}+m_1-1} + I_{03} r^{m_1+1} + I_{03,r} r^{m_1+2}$$

$$+ \sum_{n=-\infty, n\neq 0}^{\infty} \left[\begin{array}{l} (\sum_{j=1}^{4}[(in+\eta_{nj} N_{nj}-N_{nj})]B_{nj} r^{\eta_{nj}+m_1-1}) + (in)I_{n1} r^{m_1+1} + I_{n3} r^{m_1+1} + inI_{n2} r^{m_1} \\ +I_{n3,r} r^{m_1+2} \end{array} e^{in\theta} \right)]$$

(33)

To determine the constants B_{nj}, the general from of boundary conditions for displacements and stresses consider as:

$$u(a,\theta)=g_1(\theta) \qquad u(b,\theta)=g_2(\theta) \qquad v(a,\theta)=g_3(\theta) \qquad v(b,\theta)=g_4(\theta)$$

$$\sigma_{rr}(a,\theta)=g_5(\theta) \qquad \sigma_{rr}(b,\theta)=g_6(\theta) \qquad \sigma_{r\theta}(a,\theta)=g_7(\theta) \qquad \sigma_{r\theta}(b,\theta)=g_8(\theta)$$

(34)

It is recalled that Eq. (30) through Eq. (33) contain four unknowns Bn_1, Bn_2, Bn_3 and Bn_4. Therefore, four boundary conditions are required to evaluate the four unknowns. These boundary conditions may be selected from the list of conditions given in Eq. (34). Assume that the four boundary conditions are specified from the list of Eq. (34). The boundary conditions may be either the given displacements or stresses, or combinations. Expanding the given boundary conditions in complex Fourier series gives

$$g_j(\theta) = \sum_{n=-\infty}^{\infty} G_j(n) e^{in\theta} \qquad j=1,2$$

$$G_j(n) = \frac{1}{2\pi} \int_{-\pi}^{\pi} g_j(n) e^{-in\theta} d\theta \qquad j=1,2$$

(35)

Substituting the four boundary conditions (34) with the exploit of Eq. (35) in Eq. (31), Eq. (32), and Eq. (33) the constants of integration Bn_j are calculated.

3   RESULTS AND DISCUSSION

Consider a thick hollow cylinder of inner radius $a = 1m$ and outer radius $b = 1.2m$. The Poisson's ratio is assumed 0.3 and the modulus of elasticity of the inner radius is $E_i = 200Gpa$, respectively. For simplicity of analysis we consider the power law of material properties be the same as $m_1 = m_2 = m_3 = m_4 = m$ and $P = 50Mpa$.

As the first example, consider a thick hollow cylinder where the inside boundary is traction-free with given pressure distribution $\sigma_{rr}(a,\theta) = -p_i \cos 2\theta$, $\sigma_{r\theta}(a,\theta) = 0$, $\sigma_{r\theta}(b,\theta) = 0$ and $u(a,\theta) = 0$. As the second example, a thick-walled cylinder may be assumed with $\sigma_{rr}(a,\theta) = 0$, $\sigma_{r\theta}(a,\theta) = -\tau_0$, $u(a,\theta) = 0$ and $v(a,\theta) = 0$. The reason to select such boundary conditions is to examine the mathematical strength of the proposed method. These types of boundary conditions may not be handled with the potential function method. Fig. 1 shows the radial perfect plastic stress by substituting $M = 0$ in radial linear plastic stress formula in the cross section of a cylinder (example 1). The absolute maximum radial perfect plastic stresses occurs at the inner edge because of the type of boundary conditions. By substituting $M = 0$ in linear plastic stresses formula the perfect plastic stresses yields. Fig. 2 demonstrates the circumferential perfect plastic stress by substituting $M = 0$ in circumferential linear plastic stress formula in the cross section of a cylinder in the section of a cylinder (example 1). The normalized tangential stress components at the inner edge are found to be higher than those at the outer edge. Fig. 3 indicates the shear perfect plastic stress by substituting $M = 0$ in shear linear plastic stress formula in the cross section of a cylinder in the section of a cylinder (example 1). The shear perfect plastic stress components at the inner edge are found to be higher than those at the outer edge. Fig. 4 shows the radial distribution of radial perfect plastic stress by substituting $M = 0$ in radial linear plastic stress formula at $\theta = \dfrac{\pi}{3}$ (example 1). Effect of power-law index on the radial perfect plastic stress is shown in this figure. By increasing grading parameter m, the normalized radial plastic stresses at the outer section decrease in a cylinder. Fig. 5 shows the radial distribution of circumferential perfect plastic stress by substituting $M = 0$ in circumferential linear plastic stress formula at $\theta = \dfrac{\pi}{3}$ (example 1). Effect of power-law index on the circumferential plastic stress is shown in this figure. By increasing grading parameter m, the normalized circumferential plastic stresses at the outer section decrease in a cylinder. Fig. 6 indicates the radial distribution of shear perfect plastic stress by substituting $M = 0$ in shear linear plastic stress formula at $\theta = \dfrac{\pi}{3}$ (example1). Effect of power-law index on the shear perfect plastic stress is shown in this figure. By increasing grading parameter m, the normalized shear plastic stresses at the outer section decrease in a cylinder. Fig. 7 shows the radial perfect plastic stress by substituting $M = 0$ in radial linear plastic stress formula in the cross section of a cylinder (example 2). The absolute maximum radial perfect plastic stresses occur at the inner edge because of the type of boundary conditions. Fig. 8 shows the circumferential perfect plastic stress by substituting $M = 0$ in circumferential linear plastic stress formula in the section of a cylinder (example 2). The absolute maximum circumferential plastic stresses occur at the inner edge because of the type of boundary conditions. Fig. 9 shows the shear perfect plastic stress in the section of a cylinder (example 2). The absolute maximum shear plastic stresses occur at the inner edge because of the type of boundary conditions. Fig. 10 demonstrates the radial distribution of radial perfect plastic stress by substituting $M = 0$ in radial linear plastic stress formula at $\theta = \dfrac{\pi}{3}$ (example 2). Effect of power-law index on the radial plastic stress is shown in this figure. By increasing grading parameter m, the normalized radial plastic stresses at the outer section decrease in a cylinder. Fig. 11 shows the radial distribution of circumferential perfect plastic stress by substituting $M = 0$ in circumferential linear plastic stress formula at $\theta = \dfrac{\pi}{3}$ (example 2). Effect of power-law index on the circumferential plastic stress is shown in this figure. By increasing grading parameter m, the normalized circumferential plastic stresses at the outer section decrease in a cylinder. Fig. 12 shows the radial distribution of

shear perfect plastic stress at $\theta = \dfrac{\pi}{3}$ (example 2). Effect of power-law index on the shear perfect plastic stress is shown in this figure. By increasing grading parameter m, the shear perfect plastic stresses at the outer section decrease in a cylinder. Fig. 13 shows the radial linear plastic stress in the cross section of a cylinder   for $M = 0.1$ (example 1). Fig. 14 shows the circumferential linear plastic stress in the cross section of a cylinder   for $M = 0.1$ (example 1). Fig. 15 shows the shear linear plastic stress in the cross section of a cylinder   for $M = 0.1$ (example 1). Fig. 16 indicates the radial elastic stress in the cross section of a cylinder for $\varepsilon_{rr}^{p} = \varepsilon_{rr,r}^{p} = \varepsilon_{rr,rr}^{p} = 0$ (example 1). By substituting $\varepsilon_{rr}^{p} = \varepsilon_{rr,r}^{p} = \varepsilon_{rr,rr}^{p} = 0$ in linear plastic stresses formula the elastic stresses obtain. Fig. 17 indicates the circumferential elastic stress in the cross section of a cylinder for $\varepsilon_{rr}^{p} = \varepsilon_{rr,r}^{p} = \varepsilon_{rr,rr}^{p} = 0$ (example 1). By substituting $\varepsilon_{rr}^{p} = \varepsilon_{rr,r}^{p} = \varepsilon_{rr,rr}^{p} = 0$ in linear plastic stresses formula the elastic stresses obtain. Fig. 18 shows the shear elastic stress in the cross section of a cylinder for $\varepsilon_{rr}^{p} = \varepsilon_{rr,r}^{p} = \varepsilon_{rr,rr}^{p} = 0$ (example 1). By substituting $\varepsilon_{rr}^{p} = \varepsilon_{rr,r}^{p} = \varepsilon_{rr,rr}^{p} = 0$ in linear plastic stresses formula the elastic stresses obtain.
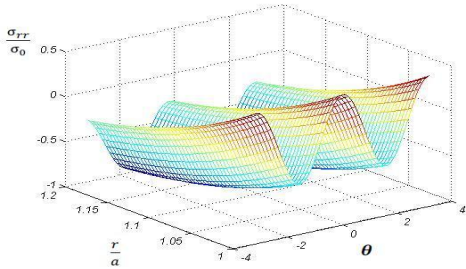
Fig.1
Radial perfect plastic stress in the cross section of a cylinder for $M = 0$ (example 1).
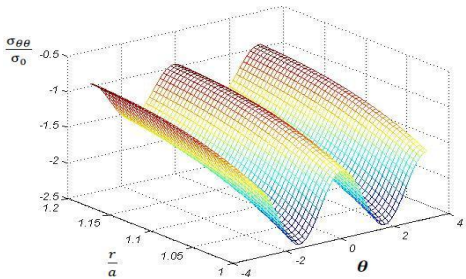
Fig.2
Circumferential perfect plastic stress in the cross section of a cylinder for $M = 0$ (example 1).
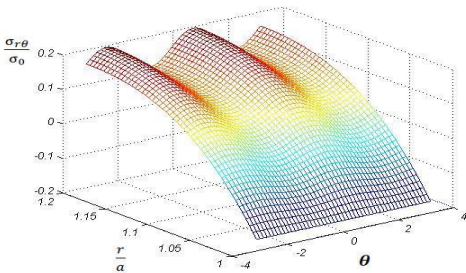
Fig.3
Shear perfect plastic stress in the cross section of a cylinder for $M = 0$ (example 1).
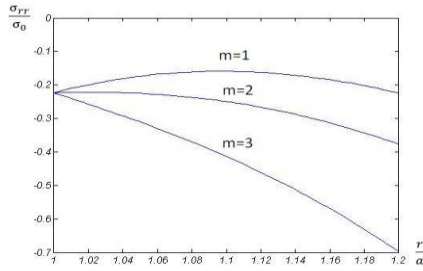
Fig.4
Radial distribution of radial perfect plastic stress for $M = 0$ at $\theta = \dfrac{\pi}{3}$ (example 1).
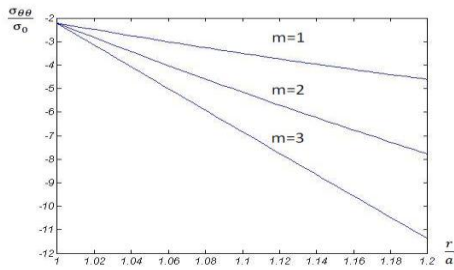
Fig.5
Radial distribution of circumferential perfect plastic stress for $M = 0$ at $\theta = \dfrac{\pi}{3}$ (example 1).
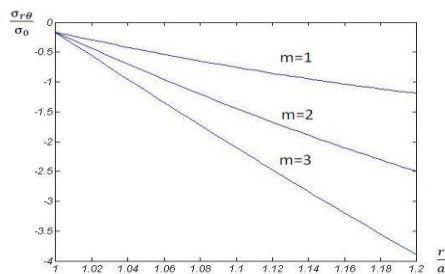
Fig.6
Radial distribution of shear perfect plastic stress for $M = 0$ at $\theta = \dfrac{\pi}{3}$ (example1).
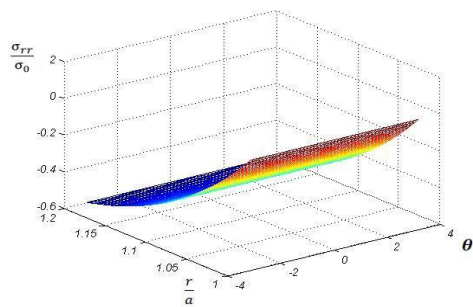
Fig.7
Radial perfect plastic stress in the cross section of a cylinder for $M = 0$ (example 2).
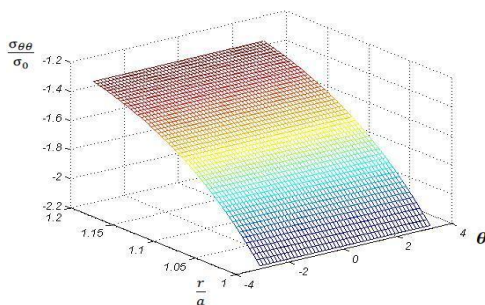
Fig.8
Circumferential perfect plastic stress in the cross section of a cylinder for $M = 0$ (example 2).
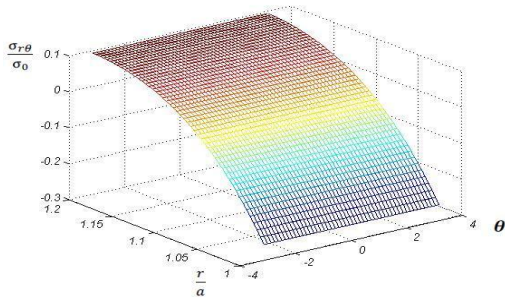
Fig.9
Shear perfect plastic stress in the cross section of a cylinder for $M = 0$ (example 2).
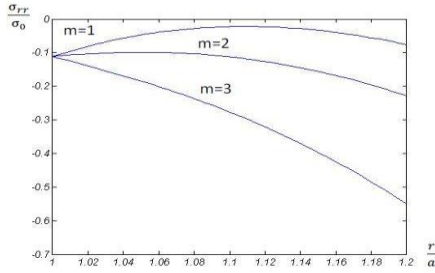
Fig.10
Radial distribution of radial perfect plastic stress for $M = 0$ at $\theta = \dfrac{\pi}{3}$ (example 2).
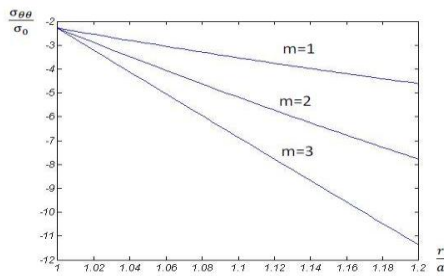
Fig.11
Radial distribution of circumferential perfect plastic stress for $M = 0$ at $\theta = \dfrac{\pi}{3}$ (example 2).
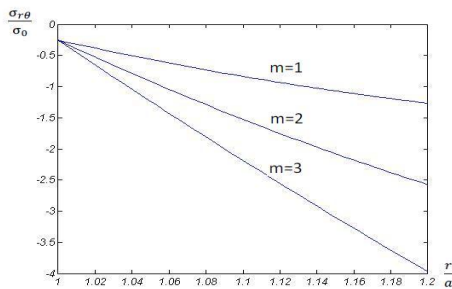
Fig.12
Radial distribution of shear perfect plastic stress for $M = 0$ at $\theta = \dfrac{\pi}{3}$ (example 2).
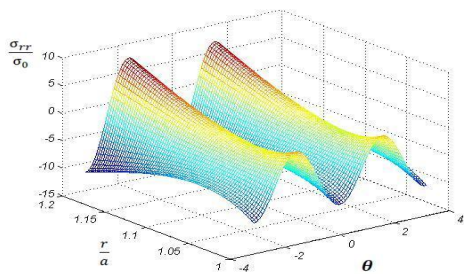
Fig.13
Radial linear plastic stress in the cross section of a cylinder for $M = 0.1$ (example 1).
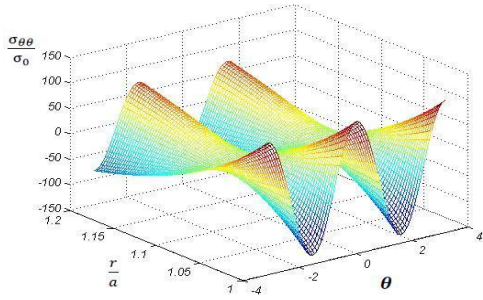
Fig.14
Circumferential linear plastic stress in the cross section of a cylinder for $M = 0.1$ (example 1).
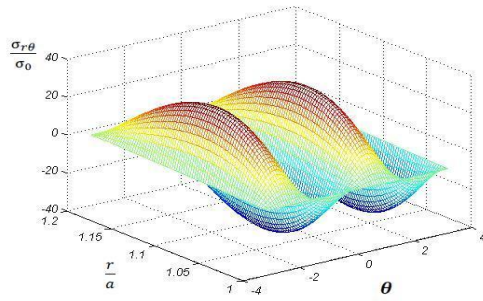
Fig.15
Shear linear plastic stress in the cross section of a cylinder for $M = 0.1$ (example 1).
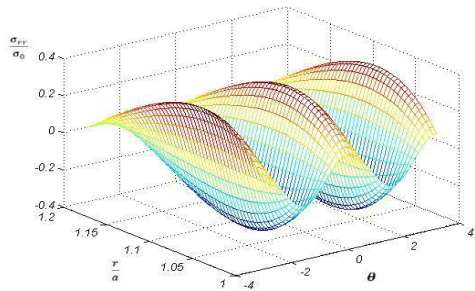
Fig.16
Radial elastic stress in the cross section of a cylinder for $\varepsilon_{rr}^p = \varepsilon_{rr,r}^p = \varepsilon_{rr,rr}^p = 0$ (example 1).
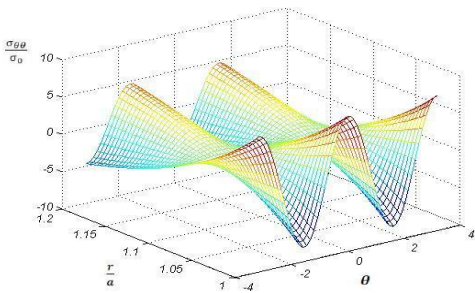
Fig.17
Circumferential elastic stress in the cross section of a cylinder for $\varepsilon_{rr}^p = \varepsilon_{rr,r}^p = \varepsilon_{rr,rr}^p = 0$ (example 1).
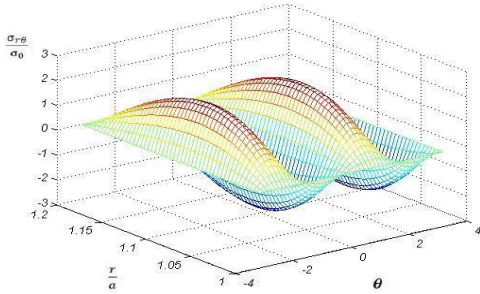
Fig.18
Shear elastic stress in the cross section of a cylinder for $\varepsilon_{rr}^{p} = \varepsilon_{rr,r}^{p} = \varepsilon_{rr,rr}^{p} = 0$ (example 1).

4   CONCLUSIONS

The analytical solution for the non-axisymmetric mechanical linear stresses in a thick hollow cylinder made of functionally graded material has been presented. The method of solution considered based on the direct method and using power series, rather than the potential function method. The advantage of this method is its mathematical power to handle mathematical function for the mechanical linear plastic stresses boundary conditions. The yield strength through the graded direction is assumed to be nonlinear with a power law distribution. Depending on applied boundary condition, by selecting optimum value of *m*, desirable level of radial and circumferential and shear stresses could be obtained in FGM cylinders with respect to those in homogenous ones. By setting $m = 0$ in every equation the radial, circumferential and shear stresses expressions turned to homogenous ones which could approve the validity of formulations. It is to be emphasized that the proposed method does not have the mathematical limitations to handle the general types of boundary conditions which are usually countered in the potential function method. Effect of power-law index on the shear plastic stress has been shown in this paper. By increasing grading parameter *m*, the normalized shear plastic stresses at the outer section decrease in a cylinder. The normalized tangential stress components at the outer edge are found to be higher than those at the inner edge. The magnitude of the tangential stress is higher than that of the radial stress. The absolute maximum radial plastic stresses occur at the inner edge because of the type of boundary conditions. By substituting $M = 0$ in linear plastic stresses formula the perfect plastic stresses have been obtained. By substituting $\varepsilon_{rr}^{p} = \varepsilon_{rr,r}^{p} = \varepsilon_{rr,rr}^{p} = 0$ in linear plastic stresses formula the elastic stresses have been yielded.

APPENDIX A

$$g_1 = m_1 + 1 \quad , \quad g_2 = \frac{vm_1}{1-v} - 1 - \frac{(1-2v)n^2}{2-2v} \quad , \quad g_3 = \frac{in}{2-2v} \quad , \quad g_4 = in\left(\frac{v(4+2m_1)-3}{2-2v}\right)$$

$$g_5 = \frac{2v-1}{1-v} \quad , \quad g_6 = \frac{2vm_1 + 4v - m_1 - 2}{1-v} - \frac{(2-2v)n^2}{1-2v} \quad , \quad g_7 = -m_1 - 1 - \frac{(2-2v)n^2}{1-2v}$$

$$g_8 = \frac{in}{1-2v} \quad , \quad g_9 = \frac{3-4v}{1-2v} + m_1 \quad , \quad g_{10} = \frac{1-3v}{1-2v} - m_1 - 1 \quad , \quad g_{11} = 2 + 2g_1 + g_2$$

$$g_{12} = g_1 + g_2 \quad , \quad g_{13} = 2g_3 + g_4 \quad , \quad g_{14} = g_3 + g_4 \quad , \quad g_{15} = 2 + 2g_1 + g_7$$

$$g_{16} = g_1 + g_7 \quad , \quad g_{17} = 2g_8 + g_9 \quad , \quad g_{18} = g_8 + g_9$$

REFERENCES

[1]   Lutz M.P., Zimmerman R.W., 1996, Thermal stresses and effective thermal expansion coefficient of functionally graded sphere, *Journal of Thermal Stresses* **19**:39-54.
[2]   Zimmerman R.W., Lutz M. P., 1999, Thermal stresses and thermal expansion in a uniformly heated functionally graded cylinder, *Journal of Thermal Stresses* **22**:177-188.
[3]   Jabbari M., Sohrabpour S., Eslami M.R., 2003, General solution for mechanical and thermal stresses in functionally graded hollow cylinder due to non-axisymmetric steady-state loads, *Journal of Applied Mechanics* **70**:111-118.

[4]   Poultangari R., Jabbari M., Eslami M.R. 2008, Functionally graded hollow spheres under non-axisymmetric thermo-mechanical loads, *International Journal of Pressure Vessels and Piping* **85**: 295-305.

[5]   Lu Y., Zhang K., Xiao J., Wen D., 1999, Thermal stresses analysis of ceramic/metal functionally gradient material cylinder, *Applied Mathematics and Mechanics* **20**(4): 413-417.

[6]   Shariyat M., Lavasani S.M.H., Khaghani M., 2010, Nonlinear transient thermal stress and elastic wave propagation analyses of thick temperature-dependent FGM cylinders, using a second-order point-collocation method**,** *Applied Mathematical Modelling* **34**:898-918.

[7]   Shariyat M., 2009, A nonlinear Hermitian transfinite element method for transient behavior analysis of hollow functionally graded cylinders with temperature-dependent materials under thermo-mechanical loads, *International Journal of Pressure Vessels and Piping* **86**: 280-289.

[8]   Lü C.F., Chen W.Q., Lim C.W., 2009, Elastic mechanical behavior of nano-scaled FGM films incorporating surface energies, *Composites Science and Technology* **69**: 1124-1130.

[9]   Afsar A.M., Sekine H., 2002, Inverse problems of material distributions for prescribed apparent fracture toughness in FGM coatings around a circular hole in infinite elastic media, *Composites Science and Technology* **62**:1063-1077.

[10]   Tajeddini V., Ohadi A., Sadighi M., 2011, Three-dimensional free vibration of variable thickness thick circular and annular isotropic and functionally graded plates on Pasternak foundation, *International Journal of Mechanical Sciences* **53**:300-308.

[11]   Nosier A., Fallah F., 2009, Nonlinear analysis of functionally graded circular plates under asymmetric transverse loading, *International Journal of Non-Linear Mechanics* **44**:928-942.

[12]   Zhang D.G., Zhou Y. H., 2008, A theoretical analysis of FGM thin plates based on physical neutral surface ,*Computational Materials Science* **44** :716-720.

[13]   Fazelzadeh S.A., Hosseini M., 2007, Aero thermo elastic behavior of supersonic rotating thin-walled beams made of functionally graded materials, *Journal of Fluids and Structures* **23**:1251-1264.

[14]   Ootao Y., Tanigawa Y., 2004, Transient thermo elastic problem of functionally graded thick strip due to Non- uniform heat supply , *Composite Structures* **63**(2):139-146.

[15]   Jabbari M., Sohrabpour S., Eslami M.R., 2002, Mechanical and thermal stresses in a functionally graded hollow cylinder due to radially symmetric loads , *International Journal of Pressure Vessels and Piping* **79**:493-497.

[16]   Farid M. , Zahedinejad P. , Malekzadeh P., 2010, Three-dimensional temperature dependent free vibration analysis of functionally graded material curved panels resting on two-parameter elastic foundation using a hybrid semi-analytic, differential quadrature method, *Materials and Design* **31**:2-13.

[17]   Bagri A., Eslami M.R., 2008, Generalized coupled thermo elasticity of functionally graded annular disk considering the Lord–Shulman theory, *Composite Structures* **83**:168-179.

[18]   Jabbari M., Bahtui A., Eslami M.R., 2009, Axisymmetric mechanical and thermal stresses in thick short length functionally graded material cylinder, *International Journal of Pressure Vessels and Piping* **86**: 296-306.

[19]   Zamani Nejad M., Rahimi G.H., 2009, Deformations and stresses in rotating FGM pressurized thick hollow cylinder under thermal load, *Scientific Research and Essay* **4**(3): 131-140.

[20]   Batra R.C., Iaccarino G.L., 2008, Exact solutions for radial deformations of a functionally graded isotropic and incompressible second-order elastic cylinder, *International Journal of Non-Linear Mechanics* **43**:383-398.

[21]   Shao Z.S., Wang T.J., 2006, Three-dimensional solutions for the stress fields in functionally graded cylindrical panel with finite length and subjected to thermal/mechanical loads, *International Journal of Solids and Structures* **43**: 3856-3874.

[22]   Shabanaa Y.M., Noda N., 2001, Thermo-elasto-plastic stresses in functionally graded materials subjected to thermal loading taking residual stresses of the fabrication process into consideration, *Composites: Part B* **32**: 111-121.

[23]   Eraslan A.N., Akis T., 2006, Plane strain analytical solutions for a functionally graded elastic–plastic pressurized tube, *International Journal of Pressure Vessels and Piping* **83**: 635-644.

[24]   Eraslan A.N., Arselan E., 2007, Plane strain analytical solutions to rotating partially plastic graded hollow shafts, *Turkish Journal of Engineering and Environmental Sciences* **31**: 273-288.

[25]   Eraslan A.N., Akis T., 2005, Elastoplastic response of a long functionally graded tube subjected to internal pressure, *Turkish Journal of Engineering and Environmental Sciences* **29**(6): 361-368.

[26]   Alla M.N., Ahmed K. I. E., Allah I. H., 2009, Elastic–plastic analysis of two-dimensional functionally graded materials under thermal loading, *International Journal of Solids and Structures* **46**: 2774-2786.

[27]   Lü H. Ç., 2011, Stress analysis in a functionally graded disc under mechanical loads and a steady state temperature distribution, *Indian Academy of Sciences Sadhana* **36**: 53-64.

[28]   Jahromi B. H., 2012, Elasto-plastic stresses in a functionally graded rotating disk, *Journal of Engineering Materials and Technology* **134**: 021004-021015.

[29]   Sadeghian M., Toussi H. E., 2012, Elasto-plastic axisymmetric thermal stress analysis of functionally graded cylindrical vessel, *Journal of Basic and Applied Scientific Research* **2**(10): 10246-10257.

[30]   Mendelson A., 1986, *Plasticity: Theory and Application*, New York, MacMillan.